OPEN ACCESS Freely available online

ISSN 2737-5323
Volume 4, Issue 1
https://www.iikii.com.sg/journal/AFM
Applied Functional Materials

Article

Integration Device of Super-Capacitors with Dye-Sensitized Solar Cells

Tung-Lung Wu [1], Kao-Wei Min [2], *, Jin-Yao Lai [3], Ming-Ta Yu [4], and Chi-Ting Ho [4]

[1] School of Mechanical and Automotive Engineering, Zhaoqing University, Zhaoqing 516260, China; tunglung216@gmail.com
[2] College of Engineering, National Formosa University, Huwei 632301, Taiwan
[3] Department of Electronic Engineering, National Formosa University, Huwei 632301, Taiwan;
[4] Department of Mechanical Design Engineering, National Formosa University, Huwei 632301, Taiwan; yumt@nfu.edu.tw (M.-T. Yu); hoct@ms25.hinet.net (C.-T. Ho)
*Corresponding author email: d0981102@gm.nfu.edu.tw

Received: Jan 24, 2024; **Revised:** Feb 24, 2024; **Accepted:** Mar 20, 2024; **Published:** Mar 30, 2024

Abstract: This study aims to create a composite supercapacitor prepared by using carbon electrodes blended with wood-derived activated carbon and monolayer graphene. The supercapacitor was integrated into dye-sensitized solar cells (DSSCs) to form a comprehensive energy system. Such a system combines the functions of solar energy conversion and storage of solar power supply systems and wearable electronic devices. In this study, the impact of gel electrolytes was investigated on the performance and long-term stability of DSSCs and supercapacitors and the characteristics of the integrated energy system. The study results revealed that the DSSCs with gel electrolytes achieved a photovoltaic conversion efficiency of 6.19%, indicating the system's potential in light energy conversion. Additionally, by serially connecting multiple integrated components, we successfully powered LEDs, which demonstrated the system's feasibility in practical applications. The findings of this study expand the application of carbon materials in energy conversion and storage and offer new avenues for developing more efficient integrated energy systems. Future efforts further enhance the efficiency and stability of the system by optimizing material combinations and system structures, which allows for widespread applications.

Keywords: Devices, Super-Capacitors, Dye-Sensitized, Solar Cells, Activated carbon

1. Introduction

The dye-sensitized solar cells (DSSCs) originated in 1976 when H. Tsubomura et al. proposed the concept of utilizing porous zinc oxide (ZnO) as the working electrode [1]. DSSCs are electrochemical cells primarily composed of a transparent conductive oxide (TCO), a working electrode, a dye, an electrolyte, and a counter electrode. However, the cell's photovoltaic conversion efficiency was only 2.5%. In 1991, Michael Grätzel, a scientist at the EPFL laboratory in Switzerland, introduced the idea of sintering nano-sized titanium dioxide (TiO_2) particles on a conductive glass substrate [2]. This method led to the creation of a nano-porous structured electrode, replacing the previous electrode. The nano-structured electrode significantly increased the surface area, allowing more dye molecules to be adsorbed onto the electrode. Combined with improved metal-organic dyes such as ruthenium (Ru) and an electrolyte solution containing I_3^--based polycarbonate, the efficiency of DSSCs reached 7.1%. DSSCs have garnered significant attention and interest from the research community due to their low-cost materials, simple fabrication processes achievable at low temperatures, and their attributes such as flexibility, color variety, and transparency. These qualities make them conducive to large-scale, cost-effective production [3]. Furthermore, DSSCs exhibit excellent photovoltaic conversion efficiency and stability. Moreover, Nazeeruddin et al. [4] and Gao et al. [5] achieved remarkable efficiency exceeding 11% by employing a dye purification procedure or utilizing novel dyes. The photoanode of DSSCs comprises nanoscale TiO_2 that has a large surface area facilitating optimal dye absorption and possessing an appropriate porous structure [6,7].

The working principle of DSSCs involves the absorption of photon energy by dye molecules, causing the transition from the ground state (D) to an excited state (D*). As the excited state is unstable, the electron is quickly injected into the conduction band of the TiO_2. The dye molecule loses an electron, which is compensated by the electrolyte, allowing electrons to flow into the conduction band of TiO_2. Eventually, these electrons enter the conductive layer, generating a current through an external circuit. Although the electrolyte is oxidized in this process, the electrons are regenerated on the platinum counter electrode, completing the cycle. In recent years, the focus of research on DSSCs has shifted towards the electrolyte due to the following reasons.

1. Traditional iodide/triiodide (I^-/I_3^-) electrolyte solutions often contain toxic organic solvents, leading to issues related to leakage and volatility that need to be addressed.
2. The stability under prolonged exposure to sunlight and thermal conditions needs improvement for practical long-term application.
3. The requirement for tight sealing increases the manufacturing cost of DSSCs.
4. Current DSSCs cannot be fabricated into flexible and large-area cells.
5. The adverse effects of organic solvents on dye adsorption.

These issues present obstacles in applications, thus necessitating research on solid-state and gel-state electrolytes of DSSCs [8].

Transparent conductive films serve as a medium for the electrons of the external circuit. The two most common types of transparent conductive films are indium-doped tin oxide (ITO) and fluorine-doped tin oxide (FTO). To effectively avoid energy loss in transmission due to poor conductivity, these films must possess high conductivity, low film resistance, and high transmittance characteristics. The film resistance is related to the series resistance, while transmittance affects light absorption and consequently the photovoltaic conversion efficiency. Therefore, transparent conductive films play a crucial role in DSSCs [9]. Moreover, since TiO2 is used as the working electrode and requires high-temperature annealing to remove organic matter, the transparent conductive film needs to maintain conductivity at high temperatures. FTO exhibits high stability and conductivity at elevated temperatures, making it the most common material for transparent conductive films of DSSCs. The versatility and efficiency of DSSCs render them promising candidates for addressing energy needs, especially in applications where conventional silicon-based solar cells may be less feasible or cost-effective. Continued research and development efforts have been put to enhance the performance and scalability of DSSCs for advancing sustainable energy technologies. In order to facilitate power supply even in the absence of illumination, we implemented a combined device consisting of DSSCs and electric double-layer capacitors, referred to as photoelectric supercapacitors in this study. During illumination, the DSSCs charged the supercapacitors, while in the absence of light, the supercapacitors discharged to supply power to the load. The longevity of supercapacitors was attributed to their utilization of physical adsorption for charge storage, which was not constrained by the irreversible phenomena inherent in chemical reactions. Consequently, supercapacitors were charged and discharged in tens of thousands of cycles, far surpassing the lifespan of conventional batteries. This characteristic makes them exceptionally well-suited for prolonged and reliable energy storage applications.

2. Materials and Methods

The preparation of TiO_2 pastes involved mixing commercial TiO_2 nanoparticles (Degussa, P25), tert-butanol, and deionized water in specific proportions at a concentration of 10wt.%. After thorough mixing, the mixture was uniformly coated onto a substrate using a doctor's blade, which was repeated to obtain the desired thickness. Once dried, the coated TiO_2 film was mechanically compressed using an automatic press machine at a pressure of 279 kg/cm^2. The compressed TiO_2 film was then air-dried at room temperature before heat treatment in a tube furnace. The heat treatment was conducted in two steps: first, heated at 150°C for 90 min to decompose organic substances, and at 450°C for 30 min to enhance the bonding of TiO_2 nanoparticles. In this experiment, the thickness of the prepared photoanode was approximately 20 µm. Finally, the photoanode was immersed in N3 dye at 50°C for 3 h to complete the preparation of the TiO_2 photoanode. In this study, platinum (Pt) was used as the material for the counter electrode. The platinum counter electrode was fabricated by cleaning the substrate thoroughly and the following methods: (a) electron-beam evaporation: using an electron-beam evaporation machine, a layer of 1 nm platinum film was deposited onto the ITO glass substrate as the counter electrode; (b) sputter coating: using a sputter coating machine, a layer of 1 nm platinum film was coated onto the ITO glass substrate as the counter electrode.

The dye involves was prepared by immersing the photoanode into a solution consisting of N3-ruthenium complex dye (N3 dye) mixed with tert-butanol. The concentration of the solution was 3×10^{-4} M, with a ratio of 1:1. The mixture was then subjected to ultrasonic agitation for 15 min to prepare the N3 dye. The gel-state electrolyte was prepared by mixing 0.1 M LiI, 0.05 M I2, 0.75 M 4-tert-butylpyridine (TBP), and 0.6 M 1-propyl-2,3-dimethylimidazolium iodide (DMPII). PVDF-HFP and PEO were mixed at a weight ratio of 3:2 to gelate the electrolyte, with a total weight of 0.2 g, resulting in a gel concentration of 15wt%. This electrolyte was prepared in 3-Methoxypropionitrile (MPN) to fabricate the highest efficiency cells, which required the use of relatively expensive ionic liquid DMPII. In the dye sensitization process, the completed working electrode was immersed into a solution consisting of N3-ruthenium complex dye (N3 dye) mixed with tert-butanol. The electrode was then placed in a 50°C oven and maintained at this temperature for 180 min. After removal from the oven, the excess dye was removed, and the electrode was dried, completing the sensitization of the photoanode. Finally, the DSSCs components were encapsulated. Firstly, two diagonal holes were drilled in the counter electrode using a drilling machine for the injection of the electrolyte. Next, to bond the photoanode and the counter electrode, a thermoplastic polymer film (SX1170^{-30}) cut into 1×2 cm^2 pieces with a 0.6×0.6 cm^2 area was used for the working region of the photoanode. These pieces were placed on a heating platform at approximately 100°C to create a sandwich structure. The silver paste was then applied to the conductive surfaces of the photoanode and counter electrode, followed by drying in an oven at 50°C. Lastly, using a syringe, the electrolyte was injected through one of the holes in the counter electrode (Figs. 1 and 2). The holes were then sealed with thermoplastic polymer film and ITO glass, completing the encapsulation of the DSSCs. The integrated device comprising an energy-storing electric double-layer supercapacitor and a dye-sensitized solar cell consisted of two main components: the DSSC and the electric double-layer supercapacitor. The fabrication process diagrams for these components are shown in Figs. 3 and 4, respectively.

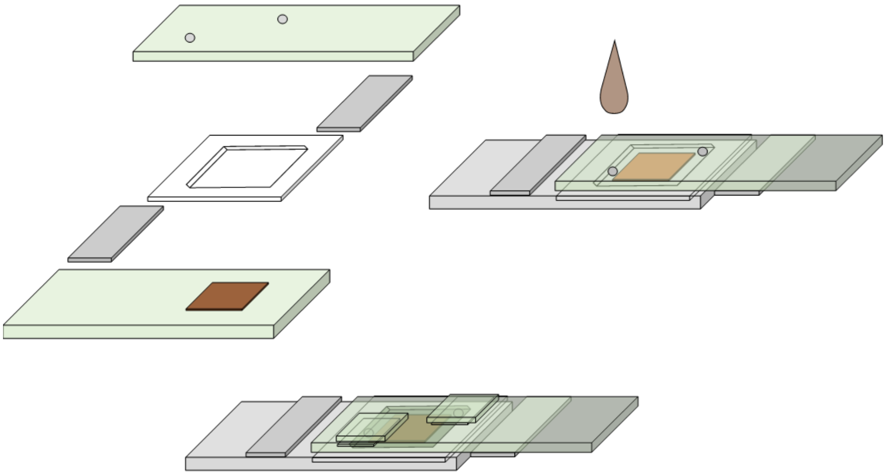

Fig. 1. Schematic diagram of DSSCs' encapsulation.

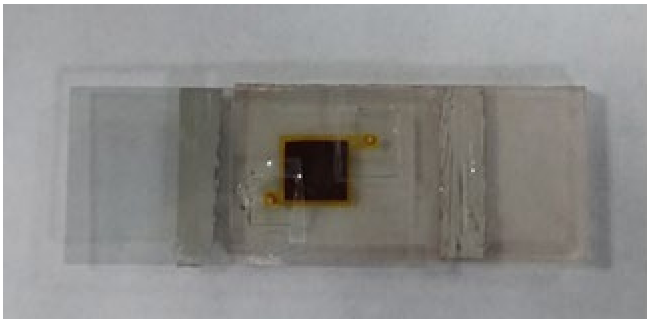

Fig. 2. Finished product of encapsulated DSSCs.

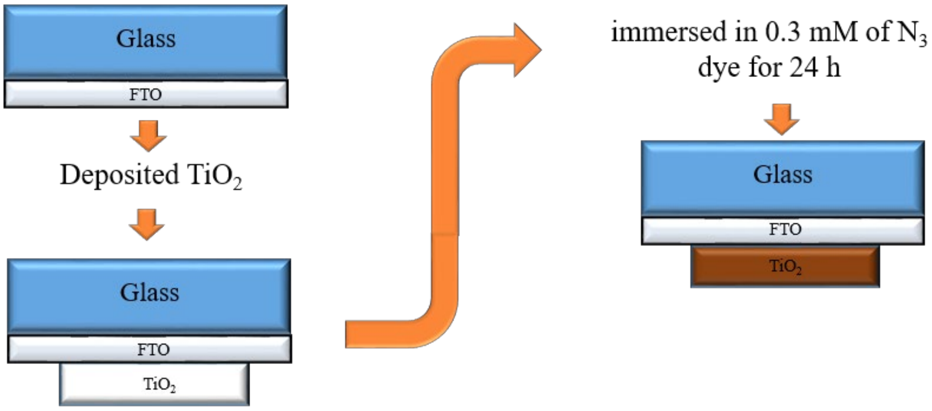

Fig. 3. Process diagram for dye-sensitized solar cell fabrication

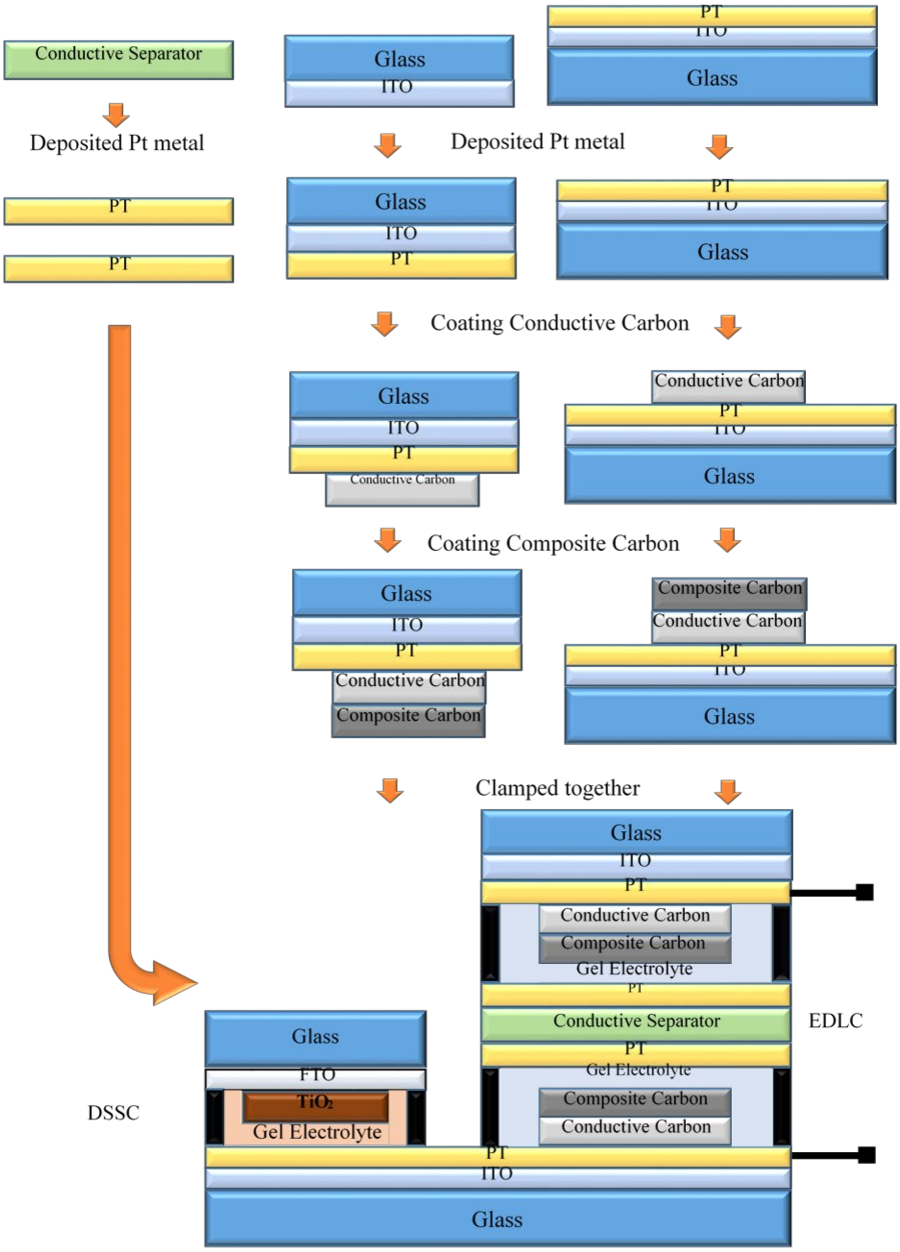

Fig. 4. Process diagram for the preparation of graphene-based supercapacitors and integration with dye-sensitized solar cell components.

The performance of the DSSC was tested using a 150W xenon lamp as the light source. The incident light was adjusted to simulate solar light AM1.5 using filters. Before measurement, the incident light intensity was adjusted to 100 mW/cm^2 at the sample position using a power meter. Subsequently, the programmable power supply Keithley 2400 was connected to the computer via KUSB-488a and controlled using LabTracer 2.0 software to regulate the output voltage. The current-voltage characteristic curve (I-V Curve) of the DSSC was then measured. The relationship between the output current (I) and output voltage (V) of a solar cell i was described by the following equation:

$$\mathrm{I} = \mathrm{I_{ph}} - \mathrm{I_o}\left\{\exp\left[\frac{q(V+R_S\mathrm{I})}{nk\mathrm{T}}\right] - 1\right\} \tag{1}$$

3. Results and Discussion

Using FE-SEM, TiO$_2$ deposited on FTO conductive glass substrates was observed. The deposition of TiO$_2$ was achieved through the blade coating method, followed by a pressurization treatment at 279 kg/cm^2, resulting in the formation of a light anode with a thickness of approximately 20 µm, as illustrated in Figure 5. Figure 6 depicts the I-V curve of the DSSC employing the gel electrolyte. It can be observed from the graph that even after one month, the DSSC maintained efficiency, indicating that the use of the gel electrolyte effectively reduced electrolyte evaporation and prolonged the lifespan of the cell. The efficiency of the DSSC is presented in Table 1. In addition to enhancing the translation and providing additional descriptive details, the effectiveness of the gel electrolyte was confirmed, which helped to prolong the cell's lifespan and maintain efficiency.

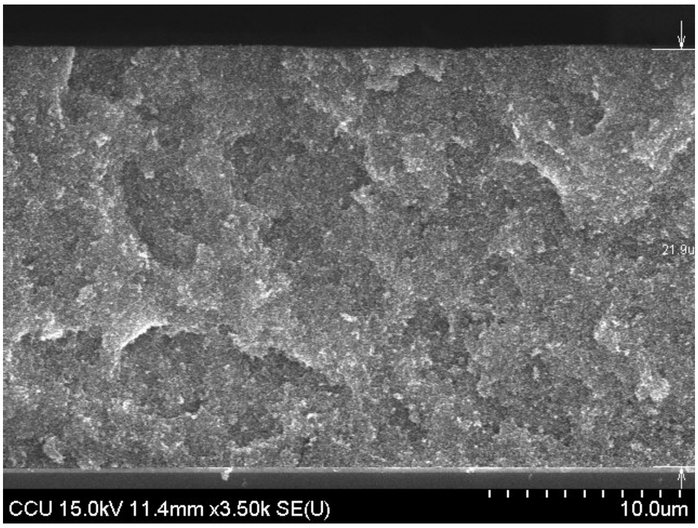

Fig. 5. FE-SEM side view of the TiO$_2$ thin film.

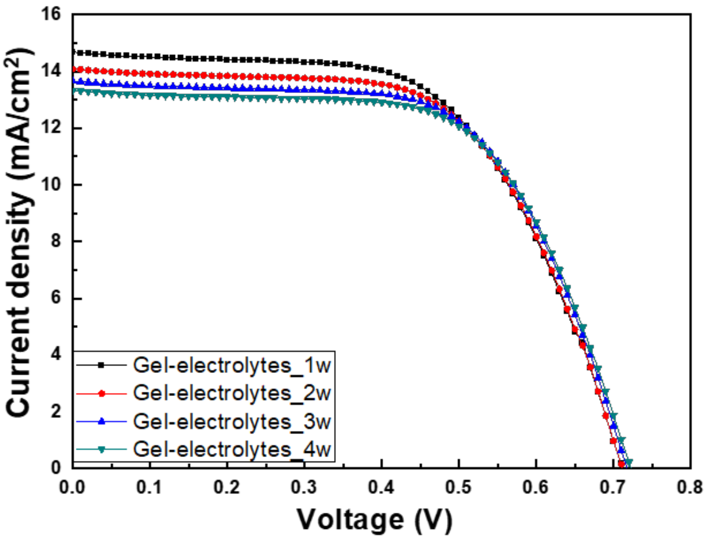

Fig. 6. Analysis of the long-term stability of DSSCs.

Table 1. Analysis of long-term stability - I-V characteristics parameters.

Sample	V_{oc} (V)	J_{sc} (mA/cm^2)	V_m (V)	J_m (mA/cm^2)	F.F (%)	η (%)
Gel-1w	0.71	14.69	0.49	12.63	59.17	6.19
Gel-2w	0.71	14.09	0.5	12.25	61.09	6.13
Gel-3w	0.72	13.66	0.51	12.02	62.50	6.13
Gel-4w	0.72	13.34	0.52	11.65	62.86	6.06

The DSSC doping with 0.07 wt.% yielded the best result. It exhibited the highest specific capacitance value of 400.3 F/g, along with a charge-discharge efficiency of 83.42% and an extended charge-discharge cycle of 885.69 seconds. Additionally, it had the largest hysteresis area, further confirming monolayer graphene as an excellent material for carbon electrodes. Next, we tested electric double-layer supercapacitors (EDLCs) for durability using the gel-state electrolyte. In order to enhance the lifespan of EDLCs, we replaced the liquid electrolyte with the gel-state electrolyte. The gel-state electrolyte used in this experiment was a 6M PVA-KOH electrolyte Despite the higher interface resistance of the liquid electrolyte, the gel-state electrolyte significantly prolonged the lifespan and effectively reduced the likelihood of electrolyte volatilization. Figure 7 shows the cyclic voltammetry (CV) test results over 500 cycles of EDLCs doped with different concentrations of monolayer graphene and the gel-state electrolyte. The EDLCs exhibited excellent capacitance retention rates. As the operating temperature increased, the gel-state electrolyte gradually liquefied, reducing the interface resistance between the electrolyte and electrodes. This increased capacitance and slowed the rate of decrease in capacitance. This indicated the successful reduction in the volatility of the gel-state electrolyte, as evidenced by the related data shown in Table 2. Figure 8 depicts the charge-discharge curves after 500 cycles of CV testing, illustrating sustained charge-discharge characteristics even after 500 cycles (Table 3).

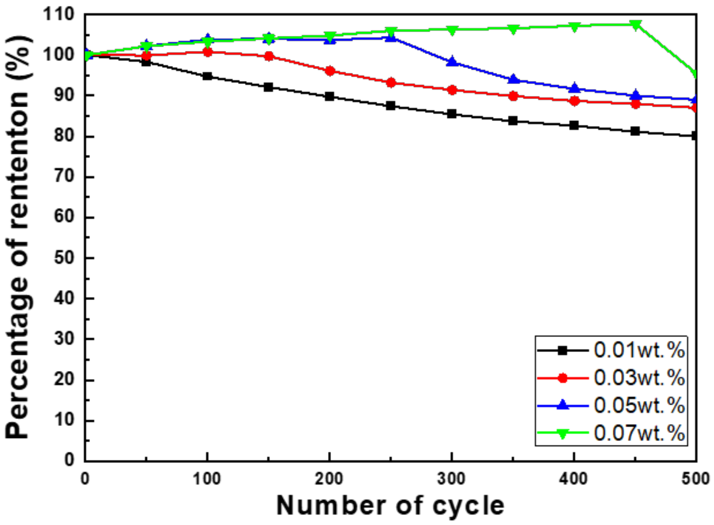

Fig. 7. Capacitance retention rates of monolayer graphene doped at different concentrations after 500 cycles of cyclic voltammetry.

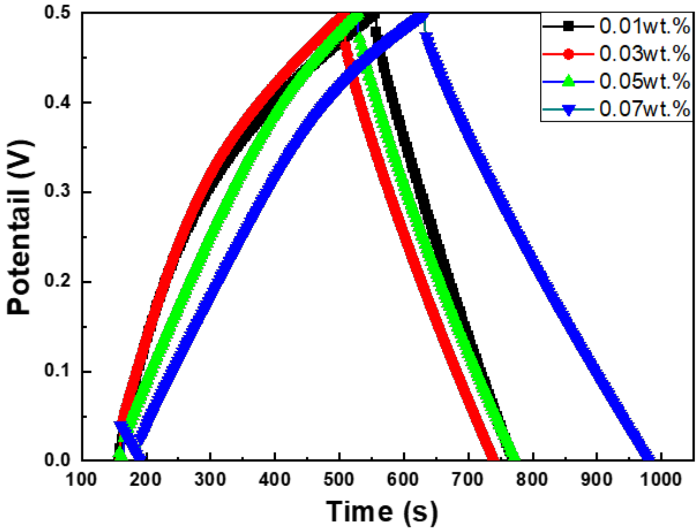

Fig. 8. Charge-discharge curves after 500 cycles of cyclic voltammetry.

Table 2. Capacitance characteristics after 500 cycles of cyclic voltammetry.

Sample	Specific capacitance (F/g)	Capacitance retention rate (%)	$\int_{V_1}^{V_2} I(V)dV$
0.01wt.%	218.08	80	1.21×10^{-2}
0.03wt.%	268.10	87	1.54×10^{-2}
0.05wt.%	293.78	89	1.85×10^{-2}
0.07wt.%	381.89	95.4	2.18×10^{-2}

Table 3. Charge-discharge characteristics after 500 cycles of cyclic voltammetry.

Sample	Charge-discharge efficiency (%)	Charge-discharge cycle (s)
0.01wt.%	64.37	500
0.03wt.%	87.46	470.5
0.05wt.%	70.23	547.8
0.07wt.%	78.15	789.1

The integrated device is used to store the electrons generated by the DSSC during illumination in EDLCs. When the light source is cut off, the EDLCs take over the power supply function. Due to the use of the gel-state electrolyte, the integrated device exhibited a long lifespan, allowing for prolonged discharge without significant self-discharge. Figure 9 illustrates the circuit diagram of the integrated device, while Figure 10 depicts the arrangement of the integrated components. Here, we conducted illumination tests for four sets of integrated components, with a red LED bulb serving as the load and a current-limiting resistor in series. In the test, the EDLCs were fully charged, and it was measured how long they powered the load until it extinguished.

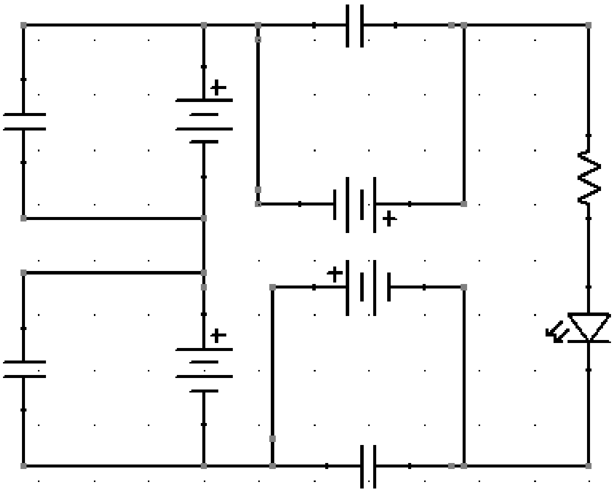

Fig. 9. Circuit diagram of the integrated device.

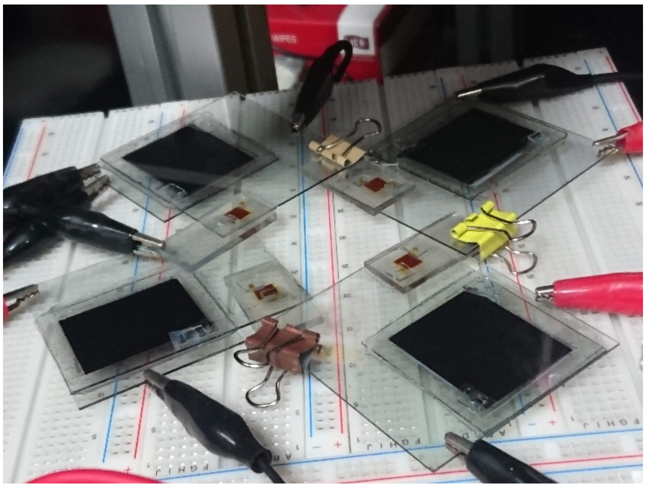

Fig. 10. Testing setup of the integrated device.

Figure 11 illustrates the process of applying the integrated device. Initially, simulated light irradiated the DSSCs, generating electrons that were then transferred to the EDLC for storage. Each EDLC was fully charged and subsequently lighted the LED bulb as shown in Fig. 11(a). Subsequently, the light source was removed, causing the DSSC to cease power supply, and the load was then powered by the EDLCs, as depicted in Fig. 11(b). After approximately 30 s, the EDLC gradually was discharged, decreasing the brightness of the LED bulb (Fig. 11(c)). Another 30 s later, the voltage of the EDLC fell below the operating voltage of the LED bulb, rendering it unable to continue lighting as shown in Fig. 11(d). If the light source was restored thereafter, the above cycle resumed, confirming the successful conversion and storage of energy in this experiment.

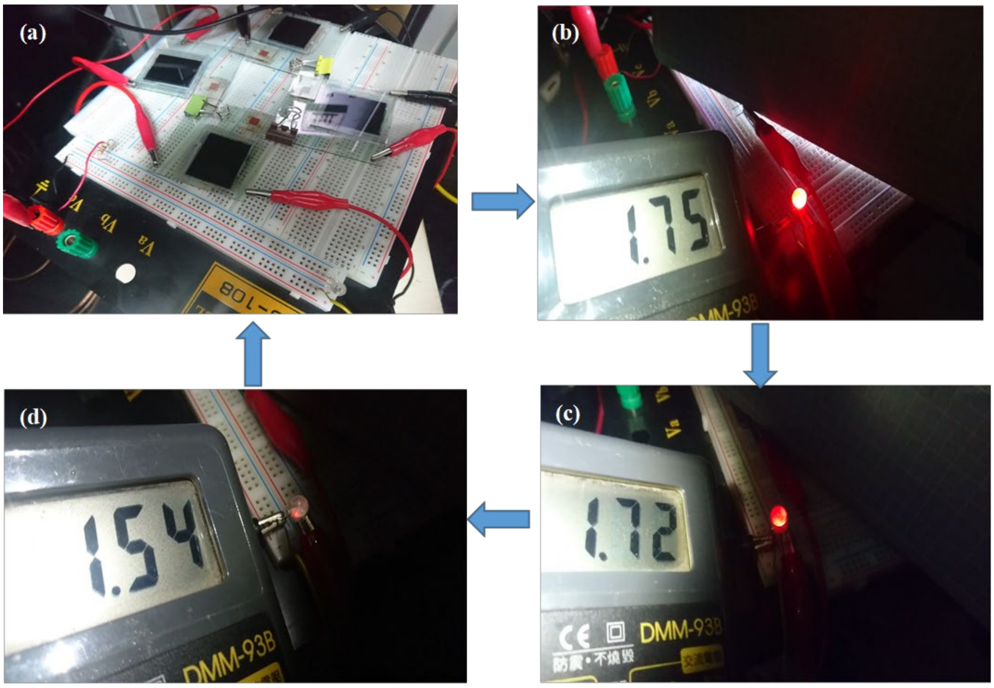

Fig. 11. Process of applying the integrated device.

4. Conclusions

Using gel-state electrolyte encapsulated DSSCs, an efficiency of 6.19% was achieved, showing no significant difference compared to the liquid counterpart. The performance was compared when using the liquid electrolyte. Even after a month, the photovoltaic conversion efficiency remained at 6.06%, indicating the excellent long-term performance of the DSSC with the gel-state electrolyte. In the 500 cycles of continuous cyclic voltammetry, 0.07 wt.% of EDLCs resulted in the best capacitance retention rate of 95.4%, with a charge-discharge efficiency of 78.15%. This demonstrates the superior long-term performance of the system, maintaining a satisfactory level of functionality over extended periods and effectively reducing the likelihood of electrolyte volatilization. We successfully integrated DSSCs with electric double-layer capacitors into a single unit, effectively combining two separate components into a system capable of simultaneously generating and storing energy. Multiple units of integrated components were connected in series and parallel to successfully power LED bulbs. Even when the light source was interrupted, the LED bulbs remained illuminated, indicating that the electrical energy was successfully stored in the electric double-layer capacitors and could continue to power the LED bulbs until depletion.

Author Contributions: conceptualization, H.-B. Tsai and C.-W. Chiu; methodology, H.-B. Tsai; validation, H.-B. Tsai and C.-W. Chiu; formal analysis, F.-Y. Liao and J.-C. Lin; investigation, C.-A. Wang and H.-T. Wu; resources, H.-B. Tsai; data curation, F.-Y. Liao and J.-C. Lin; writing—original draft preparation, H.-B. Tsai; writing—review and editing, H.-T. Wu; visualization, H.-T. Wu; supervision, H.-B. Tsai and C.-W. Chiu. All authors have read and agreed to the published version of the manuscript.

Funding: This research received no external funding.

Data Availability Statement: Not applicable.

Acknowledgments: The authors thank AR Display Co. Ltd., Taiwan for the financial support of this work.

Conflicts of Interest: The authors declare no conflict of interest.

References

1. Tsubomura, H.; Matsumura, M.; Nomura, Y.; A mamiya, T. Dye sensitised zinc oxide: aqueous electrolyte: platinum photocell. *Nature*, **1979**, *261*, 402–403.
2. O'Regan, B.; Grätzel, M. A low-cost, high-efficiency solar cell based on dye-sensitized colloidal TiO_2 films. *Nature*, **1991**, *353*, 737–740.
3. Grätzel, M.; Conversion of Sunlight to Electric Power by Nanocrystalline Dye Sensitized Solar Cells. *Journal of Photochemistry and Photobiology A: Chemistry*. **2004**, *164*, 3–18.

4. Nazeeruddin, M.K.; Angelis, F.D.; Fantacci, S.; Selloni, A.; Viscardi, G.; Liska, P.; Ito, S.; Takeru, B.; Grätzel, M. J. Am. Dye Regeneration Kinetics of Sensitized Nickel Oxide Films under Illumination Investigated by Scanning Electrochemical Microscopy, *Chem. Soc.* **2005**, *127*, 16835–16847.
5. Gao, F.; Wang, Y.; Shi, D.; Zhang, J.; Wang, M.; Jing, X.; Baker, R.H.; Wang, P.; Zakeeruddin, S.M.; Grätzel, M. Enhance the Optical Absorptivity of Nanocrystalline TiO_2 Film with High Molar Extinction Coefficient Ruthenium Sensitizers for High Performance Dye-Sensitized Solar Cells. *Journal of the American Chemical Society*, **2008**, *130*, 10720–10728.
6. Yu, D.; Zhu, X.; Xu, Z.; Zhong, X.; Gui, Q.; Song, Y.; Zhang, S.; Chen, X.; Li, D. Facile Method to Enhance the Adhesion of TiO_2 Nanotube Arrays to Ti Substrate. *ACS Appl. Mater. Interfaces*, **2014**, *6*, 8001–8005.
7. Kim, C.; Kim, S.; Lee, J.; Kim, J.; Yoon, J. Capacitive and Oxidant Generating Properties of Black-Colored TiO_2 Nanotube Array Fabricated by Electrochemical Self-Doping. *ACS Appl. Mater. Interfaces*, **2015**, *7*, 7486–7491.
8. Iijima, S. Helical microtubules of graphitic carbon. *Nature*, **1991**, *354*, 56–58.
9. Yanagida, M. Charge transport in DSSC. *Adv. Nat. Sci: Nanosci. Nanotechnol*, **2015**, *6*, 015010.